UNIVERSITY OF CALIFORNIA SAN DIEGO

Blood Retinal Barrier Breakdown in the Long Oxygen Induced Retinopathy Mouse Model

A Thesis submitted in partial satisfaction of the requirements
for the degree Master of Science

in

Biology

by

Everett Han

Committee in charge:

Professor Richard Daneman, Chair
Professor Yunde Zhao, Co-Chair
Professor Eric Nudleman
Professor Ella Tour

2024

The Thesis of Everett Han is approved, and it is acceptable in quality and form for publication on microfilm and electronically.

University of California San Diego

2024

TABLE OF CONTENTS

Thesis Approval Page iii

Table of Contents iv

List of Figures v

Acknowledgements vi

Abstract of the Thesis vii

Introduction 1

Methods 4

Results 9

Discussion 16

References 20

LIST OF FIGURES

Figure 1: The representative normoxic, s-OIR, and l-OIR retinas of mice.....10
Figure 2: Comparison of leakage trends across normoxic, s-OIR, and l-OIR treated mice.....12
Figure 3: Leakage intensity at P23 and P30 for retinas with and without a fibrotic scar. 14

ACKNOWLEDGEMENTS

Figures 1, 2, and 3 are being prepared for submission for publication. Nudleman, Eric; Daneman, Richard. The dissertation author is the primary author and researcher of this material.

ABSTRACT OF THE THESIS

Blood Retinal Barrier Breakdown in the Long Oxygen Induced Retinopathy Mouse Model

by

Everett Han

Master of Science in Biology

University of California San Diego, 2024

Professor Richard Daneman, Chair
Professor Yunde Zhao, Co-Chair

Human retinal vasculopathies commonly result in breakdown of the blood retinal barrier and formation of scars on the retinal surface. The formation of rigid scar tissue creates traction on the retinal layers that can result in tearing, detachment, and complete blindness. Currently, the only treatment option for retinal fibrosis is surgical removal, an invasive procedure that lacks consistent success at treating the condition. Furthermore, an optimized animal model for retinal

fibrosis has yet to be developed. The absence of an animal model severely limits the improvement of patient standard of care. This creates a strong need for a model capable of emulating the clinical progression of retinal fibrosis in a laboratory setting. Mouse models have been proven effective at modeling the angiogenic features of retinal vasculopathies. However, current models have yet to produce the long-term scarring that is also present in a variety of ischemic retinal vasculopathies. Therefore, this study focuses on the scarring and leakage induced by the long oxygen induced retinopathy (l-OIR) as it compares to the classical oxygen induced retinopathy model, referred to as the standard-oxygen induced retinopathy (s-OIR) model. This study primarily focuses on how breakdown of the blood retinal barrier contributes to disease pathophysiology. This was accomplished through an extensive set of leakage assays that follow the disease progression in the mice across an array of time points. It was observed that leakage occurs immediately upon completion of the high oxygen treatment in the l-OIR model. This leakage persists for 7 days and was no longer observed at 14 days. While the s-OIR model leads to a greater acute peak in leakage, the l-OIR model produces leakage over a longer duration as well as a defined fibrotic plaque. This difference may be due to the difference in induced disease severity across the models, with l-OIR producing retinas with more damaged vascular structures, often lacking in central veins and arteries. Furthering scientific and clinical understanding of the role that leakage and scarring play in ischemic retinal vasculopathies will allow future research into bettering the standard of care for patients suffering from such diseases.

Introduction

A critical part of survival is the ability to regenerate tissue and recover from injury. Often, physical injury can impair the ability for a tissue or organ to function. Therefore, the human body possesses various mechanisms for physical and structural repair. One such mechanism is fibrosis, where rigid, durable connective scar tissue replaces the parenchymal tissue found at the site of injury. Typically, fibrosis occurs as a response to injuries characterized by chronic inflammation. These types of injuries persist for up to months where the immune response, inflammation, and tissue repair must occur concurrently.[1] While fibrosis is a natural and often beneficial part of the healing process, it can become pathogenic when not properly controlled. In these cases, an excess of extracellular matrix proteins, primarily Collagen 1 (Col1), is deposited causing the permanent replacement of normal tissue with scar tissue.[2] In the case of the retina, which is primarily delicate and highly specialized neuronal tissue, this can prove highly detrimental.

Retinal fibrosis is a feature common to a multitude of blinding eye diseases, including but not limited to proliferative diabetic retinopathy, retinopathy of prematurity, and proliferative vitreoretinopathy and is the most common cause of irreparable loss of vision in patients.[3] These diseases are ischemic retinal vasculopathies – a condition involving retinal blood vessels that results in reduced blood flow and tissue hypoxia. This spurs rapid and aberrant neovascularization, which for delicate tissue such as the retina, can be highly detrimental. Under healthy conditions the retinal vasculature possesses specialized barrier properties, referred to as the blood retinal barrier, that tightly regulates the passage of small molecules and cells into the retina.[4] However, the newly growing and immature vessels lack these barrier properties. Consequently, the retinal tissue experiences leakage of fluid, resulting in inflammation, tissue

damage, and the subsequent development of a fibrotic scar.[5] This fibrotic scar, composed primarily of Col 1, forms a rigid membrane that produces traction on the retinal surface. This traction can lead to retinal tears, holes, and detachments. As a result, patients can experience visual impairment and even complete blindness.[1] Currently, the only treatment options available are surgical and invasive, which results in limited success at treating the condition.[6] Despite the high morbidity and risks it poses to patient vision, very little is understood regarding the mechanisms that drive retinal fibrosis. As a result, treatments have remained extremely limited and the development of new therapies slow.[7] This creates the need for further research into the pathophysiology of retinal fibrosis as well as the molecular progression of the disease state.

The current model for retinal vasculopathies, the oxygen-induced retinopathy mouse model, is widely used to study the aberrant angiogenesis and associated leakage observed in human clinical cases.[8] The oxygen-induced retinopathy model induces ischemic vascular disease by mimicking the human clinical conditions of retinopathy of prematurity (ROP). Retinopathy of prematurity is a retinal condition that affects prematurely born infants.[9] The human retina is one of the last tissues to develop during gestation, estimated to mature fully around the 36-40th week of gestation.[10] Therefore, upon premature birth, the retina must continue to develop. However, because prematurely born infants are usually given supplemental oxygen to increase vitality, the development of the retinal vasculature often can be delayed due to the already abundant blood oxygen. This creates a paradoxical hypoxia in the retina whereby, upon ceasing supplemental oxygen treatment, the retina begins to rapidly neovascularize. Such neovascularization results in damaging leakage within the retina and subsequent fibrosis.[11] Such retinal fibrosis leads to the formation of a scar that binds to the vitreous, creating traction that can tear and detach the retina, leading to blindness. By mimicking the hyperoxic environment in which prematurely born

human infants are placed, the oxygen-induced retinopathy model causes a similar retinal angiogenesis in mice. The oxygen-induced retinopathy model places mice in a hyperoxic environment beginning on day 7 after birth, until day 12.[8] This leads to the characteristic pathological angiogenesis of human ocular diseases, but lacks in the clinical long-term severity observed in these diseases as the mouse retinal vasculatures recover and do not show scarring that is observed in severe ROP cases.[12] It is hypothesized that the limitations of and lack of scar formation in the oxygen-induced retinopathy model are due to the later age at which the mice are treated with high oxygen as well as the shorter duration of the treatment. Thus, by more closely simulating ROP and treating the mice with high oxygen much earlier and for a longer duration, a more optimal model for both the aberrant angiogenesis and long-term scarring was developed. The long oxygen-induced retinopathy (l-OIR) model mouse model more closely mimics the conditions of ROP by placing mice in a hyperoxic environment at day 2 after birth, until day 16. The development of a model capable of emulating the clinical progression of retinal fibrosis is critical to the advancement of medical understanding as well as improvement of patient standard of care regarding this disease.[13] This study is focused on assessing the efficacy of the l-OIR model at inducing retinal angiogenesis and scarring, in addition to the relationship between angiogenesis, leakage, and the formation of long-term scars through a series of sulfo-NHS-biotin leakage assays.

Methods

Mouse Husbandry and Litter Management

Wild type mouse colonies of strain C57/BI6 were obtained from the Jackson Laboratory (The Jackson Laboratory, Bar Harbor, ME). and managed on a standard kibble diet. Colonies were checked daily to accurately record births. Litter age was measured in days.

Standard-Oxygen induced Retinopathy (s-OIR)

The mouse oxygen induced retinopathy model, referred to in this study as the standard-oxygen induced retinopathy model (s-OIR), was performed using guidance from the Smith protocol.[8] Beginning at post-natal day 7 (P7), the litters of pups, including their mothers, were placed in a closed chamber of 75% atmospheric oxygen (Biospherix, Parish, NY, USA). At P12, the litters were removed from the chamber and returned to room air. Analysis was performed on retinas obtained from OIR treated pups of ages P12, P17, and P25.

Long-oxygen Induced Retinopathy (l-OIR)

Beginning at post-natal day 2 (P2), the litters of pups, including their mothers, were placed in a closed chamber of 75% atmospheric oxygen (Biospherix, Parish, NY, USA). Each mother of an l-OIR litter is paired with a surrogate mother of a litter maintained in room air. Every other day the mothers are switched between litters to mitigate the effects of oxygen toxicity. At P16, the litter is removed from the chamber and returned to room air. Analysis was performed on retinas obtained from l-OIR treated pups of ages P16, P19, P23, and P30.

Reagents

- 1xDPBS: 1x Dulbecco's phosphate buffered saline (Thermo Fisher Scientific, Waltham, MA, USA)
- 4% paraformaldehyde (PFA): made by combining 32% PFA (Electron Microscopy Sciences, Hatfield, PA, USA), 10x PBS {Thermo Fisher Scientific, Waltham, MA, USA), and MilliQ water (Millipore Sigma, Burlington, MA, USA). Solution was stored at 4^{o}C.
- Blocking Buffer: 0.2% Bovine Serum Albumin (Sigma-Aldrich, Burlington, MA, USA), 0.3% Triton X-100 (Sigma-Aldrich, Burlington, MA, USA), 5% Normal Goat Serum (Life Technologies, Carlsbad, CA, USA), in antibody buffer.
- Antibody buffer: 150 mM NaCl (Fisher Scientific, Fair Lawn, NJ, USA), 1% BSA, 50 microM Tris-Base (Fisher Scientific, Fair Lawn, NJ, USA), 100 microM L-lysine (Sigma-Aldrich, Burlington, MA, USA), 0.02% sodium azide (Fisher Scientific, Fair Lawn, NJ, USA), in MilliQ water. Filtered through a 0.22 microM filter and stored at 4 degrees Celsius.
- Ketamine/Xylazine: An anesthetic solution of ketamine at concentration 4mg/mL (MWI/Vetone, Boise, ID, USA) and xylazine at concentration 0.6mg/mL (MWI/Vetone, Boise, ID, USA) was used.

Perfusion

Mice were anesthetized using a solution of 4mg/ml ketamine and 0.6mg/ml xylazine at a dose of 60 microliters per gram of bodyweight. This was followed by fixation via intracardiac perfusion utilizing a Dynamax RP-1 peristaltic pump (Mettler Toledo-Rainin, Oakland, CA) at a

flow rate of approximately 4.0-4.5 mL/min. Perfusions consisted of two intervals. First mice were perfused for 10 minutes with 1xDPBS containing sulfo-NHS-biotin at a concentration of 1mg/5mL. Second, mice were perfused for 10 minutes with 4% PFA. Between perfusion of each mouse, the pump tubing was washed for 5 minutes using DPBS. Following perfusion, the eyes of each mouse were enucleated and placed in 4% PFA to incubate for 15 minutes at room temperature, after which they were stored on ice until dissection.

Fluorescent stains

Primary antibodies: rat-anti-mouse CD31 (BD Biosciences, San Jose, CA, USA) diluted to 1:500 in antibody buffer.

Secondary antibodies: goat-anti-rat 488 and streptavidin 647 (Thermo Fisher Scientific, Waltham, MA, USA) diluted to 1:1000 in antibody buffer.

Dissections and immunostaining

Using a dissecting microscope, eyes were dissected and whole retinas isolated on a 100mm x 15mm petri dish (Thermo Fisher Scientific, Waltham, MA, USA) containing 1x PBS. Two #5 forceps (FST by Dumont, Switzerland) and a 25 gauge needle (BD Biosciences, San Jose, CA, USA) were used for the dissections.

Immediately after isolation, retinas were placed in a 48-well plate (Corning, Corning, NY, USA) containing blocking buffer, wrapped in aluminum foil, and incubated overnight. The retinas and well plate would remain wrapped in aluminum foil for every step of the immunostaining. The following day, the blocking buffer was removed, the retinas were washed in 1x PBS for 5 minutes and placed in primary antibody to incubate for two days. After the two

days, the primary antibody was removed, and the retinas were washed for 3 cycles of 5 minutes in 1xPBS and placed in secondary antibody to incubate for a day. Finally, the secondary antibody was removed, and the retinas were washed for 5 minutes in 1xPBS and flat mounted.

Flat mounting

Under a dissection microscope, the retinas were placed, with the inside facing upward, on a 25x75x1mm microscope slide (VWR, Radnor, PA, USA). Two brushes and a straight-edge razor were used to cut the retinas into four leaflets, joined at the center, and flatten the tissue onto the slide. Retinas were mounted using fluoromount G with DAPI (Electron Microscopy Sciences, Hatfield, PA, USA) and covered with a glass coverslip (VWR, Radnor, PA, USA).

Imaging

Samples were imaged using a Zeiss Axio Imager M.2 with a Zeiss Axiocam 712 (Carl Zeiss AG, Oberkochen, Germany). Intensity was measured through secondary staining with streptavidin 647 and taken at an exposure of 40ms

Quantification

Quantifications were performed using ImageJ FIJI software. Intensity of streptavidin 647 signal was measured in mean grey scale value of the isolated far-red channel.

Statistical Analysis and figure generation

Leakage data organization and quantifications were performed in Microsoft Excel and were imported into GraphPad Prism where further statistics and figure generation was accomplished. A two-tailed, unpaired t-test was used to determine significance between the s-

OIR and l-OIR groups versus their respective age-matched normoxic group. Graphics of the flat-mounts and leaflets were generated using Adobe Illustrator.

Results

Leakage assays using Sulfo-NHS-Biotin and streptavidin 647 were performed to analyze the integrity of the blood retinal barrier during severe retinal ischemic vasculopathy in mice. Statistical analysis compares the treated groups (l-OIR and s-OIR) to their corresponding age-matched normoxic group. The primary focus of the study was to determine if the l-OIR model induces leakage, what stages in the disease progression does the retina leak, and how this compares to the s-OIR model.

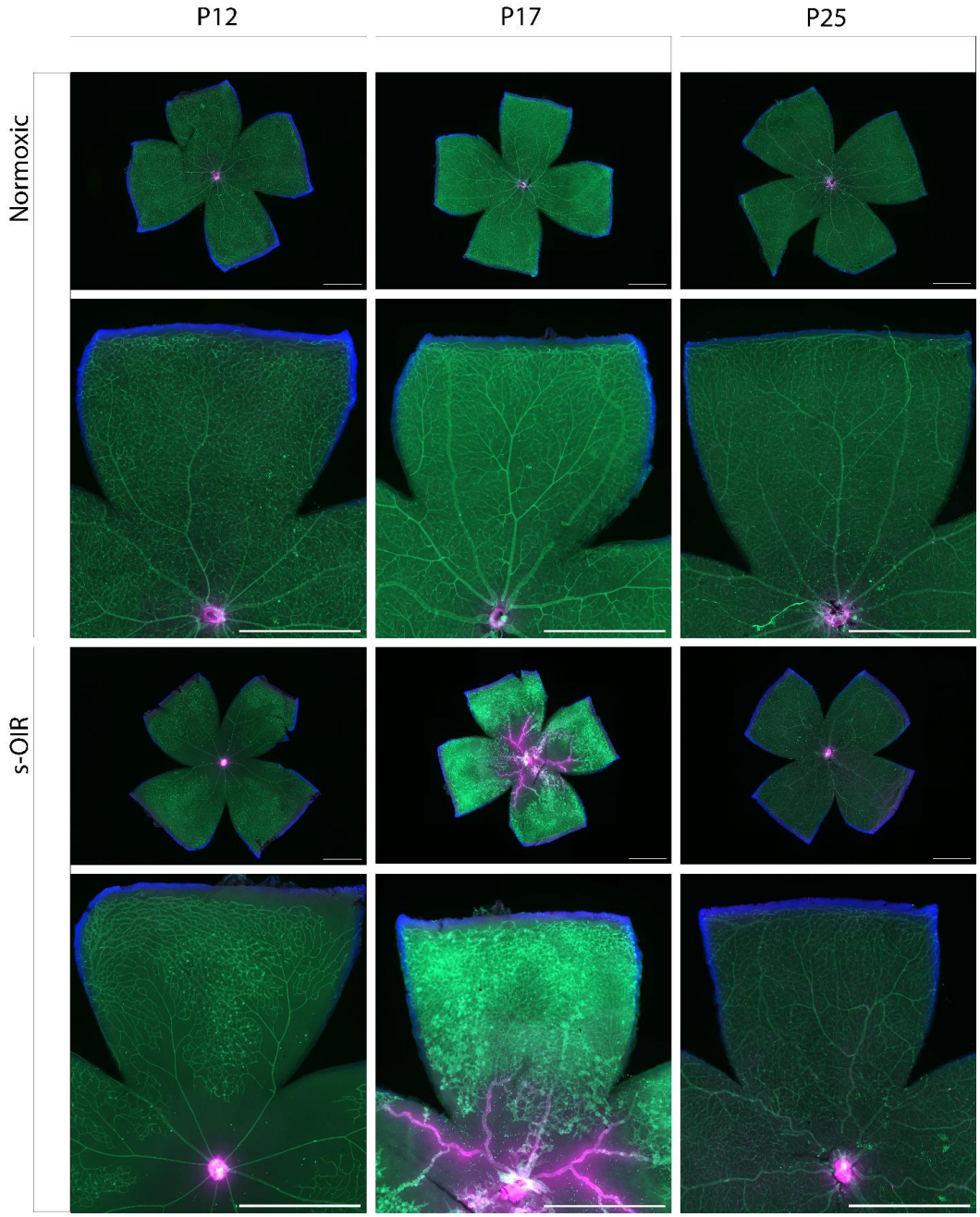

Figure 1: The representative normoxic, s-OIR, and l-OIR retinas of mice. Leakage assays were performed via intracardiac perfusion of sulfo-NHS-biotin with subsequent sectioning of the retinas. The retinas were then stained with CD31 (in green) to show the vasculature, DAPI (in blue) to visualize the cell nuclei, and streptavidin (in purple) to show the leakage of biotin. P17 s-OIR serves as the positive control and shows a large amount of streptavidin fluorescence, indicating the presence of strong leakage. The severe damage l-OIR causes to the vascular structure of the retina is shown in the l-OIR images. There is vaso-obliteration across the entire retina, including obliteration of the central veins and arteries. The fibrotic plaque is visible as the opaque membrane present in the central region of the P23 and P30 l-OIR retinas. Scale bars represent 1000 micrometers.

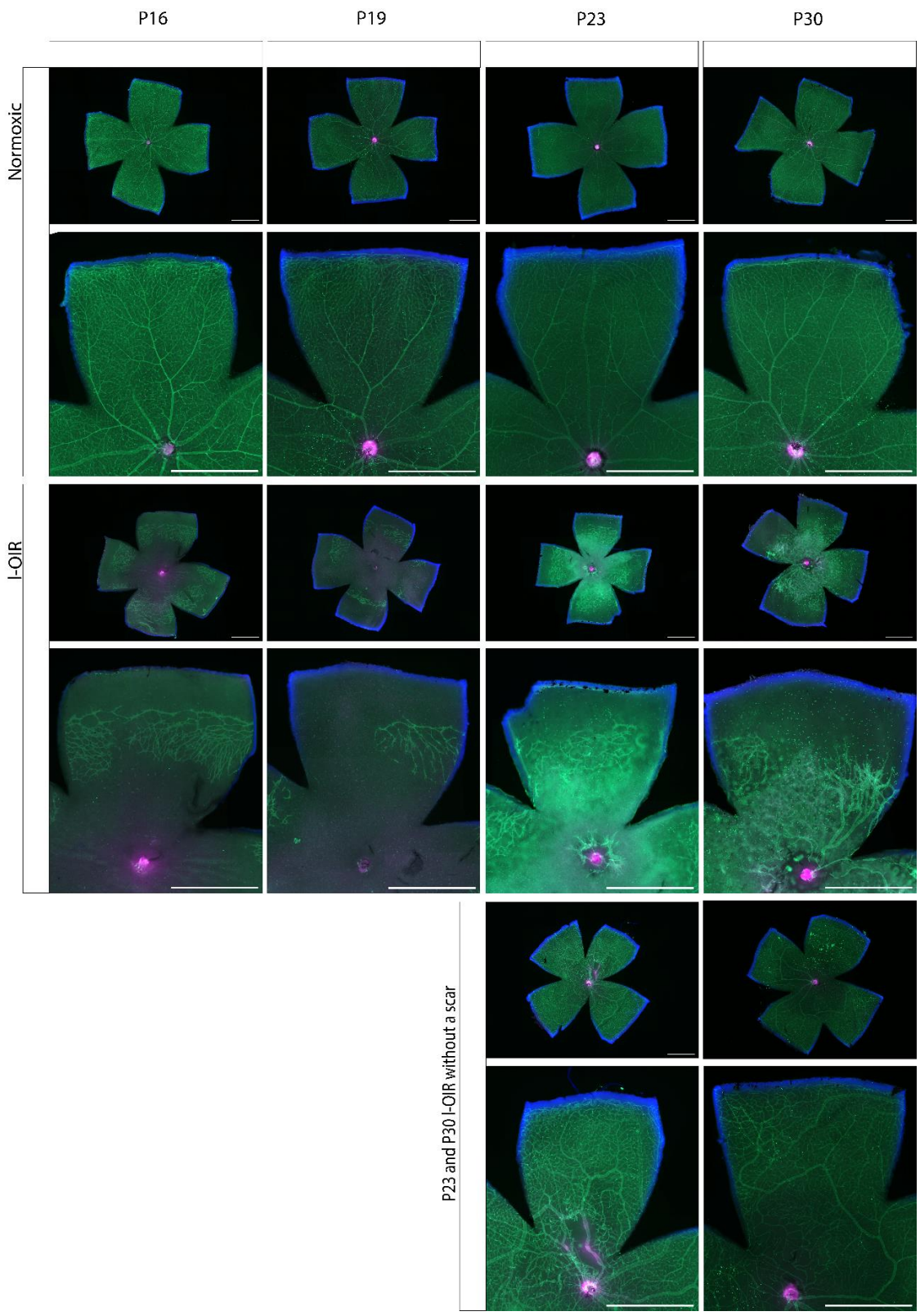

Figure 1: The representative normoxic, s-OIR, and l-OIR retinas of mice continued.

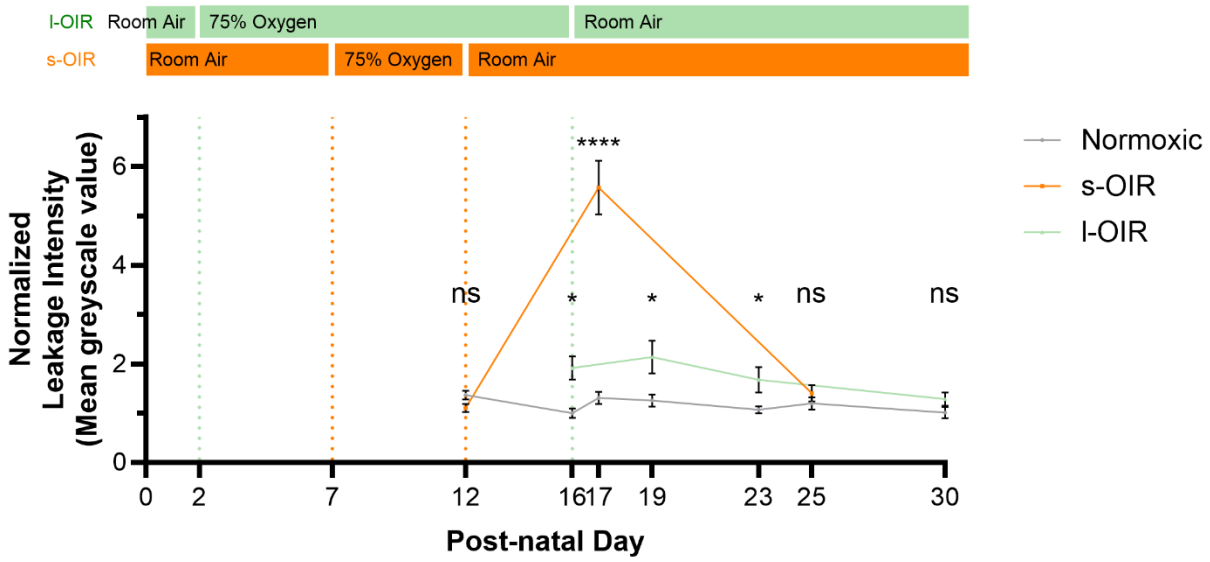

Figure 2: Comparison of leakage trends across normoxic, s-OIR, and l-OIR treated mice. The relative leakage intensities of the sample retinas, measured in mean greyscale value, were normalized to P16 normoxic and are shown across the three treatment groups of mice. It can be seen how P17 s-OIR produces an acute peak in leakage whereas l-OIR shows a much more long-term form of leakage. Statistical significance was determined through an unpaired t-test between the experimental group (s-OIR or l-OIR) and the age-matched normoxic group at the timepoint. Error bars represent 1 SEM. *$p<0.05$; ****$p<0.0001$. P12 normoxic n=10. P12 s-OIR n=13. P16 normoxic n=18. P16 l-OIR n=16. P17 normoxic n= 17. P17 s-OIR n=18. P19 normoxic n= 16. P19 l-OIR n=17. P23 normoxic n=20. P23 l-OIR n=16. P25 normoxic n=18. P25 s-OIR n=17. P30 normoxic n=18. P30 l-OIR n=25.

Establishing a positive control. To establish a positive control for the leakage assays, wild type mice were treated according to the s-OIR model and grown to post-natal day 17 (P17). The mice were then perfused using sulfo-NHS-biotin followed by PFA. Under healthy conditions, the blood retina barrier prevents small molecules, including sulfo-NHS-biotin, from leaking into the retina. During disease, however, the barrier properties break down and small

molecules penetrate the barrier. At P17, the s-OIR treated mice showed a highly significant amount of leakage compared to the P17 normoxic mice.

Leakage is not present in the early and late stages of s-OIR. To assess leakage in the s-OIR model as it correlates to disease progression, mice were treated in accordance with the s-OIR model and allowed to grow to P12, P17, and P25. Despite the leakage present at P17 in s-OIR treated mice, leakage was neither observed at P12, the first day out of hyperoxia, nor at P25.

There is leakage during the early and intermediate disease stages of l-OIR. To assess leakage as it correlates to disease progression in the l-OIR model, leakage assays were performed on mice at P16, P19, P23, and P30. Contrary to what was observed with the s-OIR model, leakage began upon the first day that the mice were removed from hyperoxia, P16. The retinal tissue would continue to leak through P19, prior to the scar forming period, as well as at P23, following scar formation. At P30, the amount of detected biotin was no longer statistically significant, indicating recovery of the blood retinal barrier.

Mice treated with l-OIR show a greater duration and consistency of leakage whereas those treated with s-OIR show a stronger acute peak in leakage. Across the actively leaking l-OIR P16, P19, and P23 timepoints, the leakage intensity remains relatively similar. Whereas the mice treated with s-OIR show a sharp peak in leakage at age P17, greater than that of any of the l-OIR treated mice, but no leakage at the ages P12 and P25. However, the s-OIR mice do not show the same consistency of leakage as the l-OIR mice. This indicates that, while the leakage intensity may be lower in l-OIR, the vasculature of the l-OIR treated mice recover slower, signifying a more chronic disease pathology.

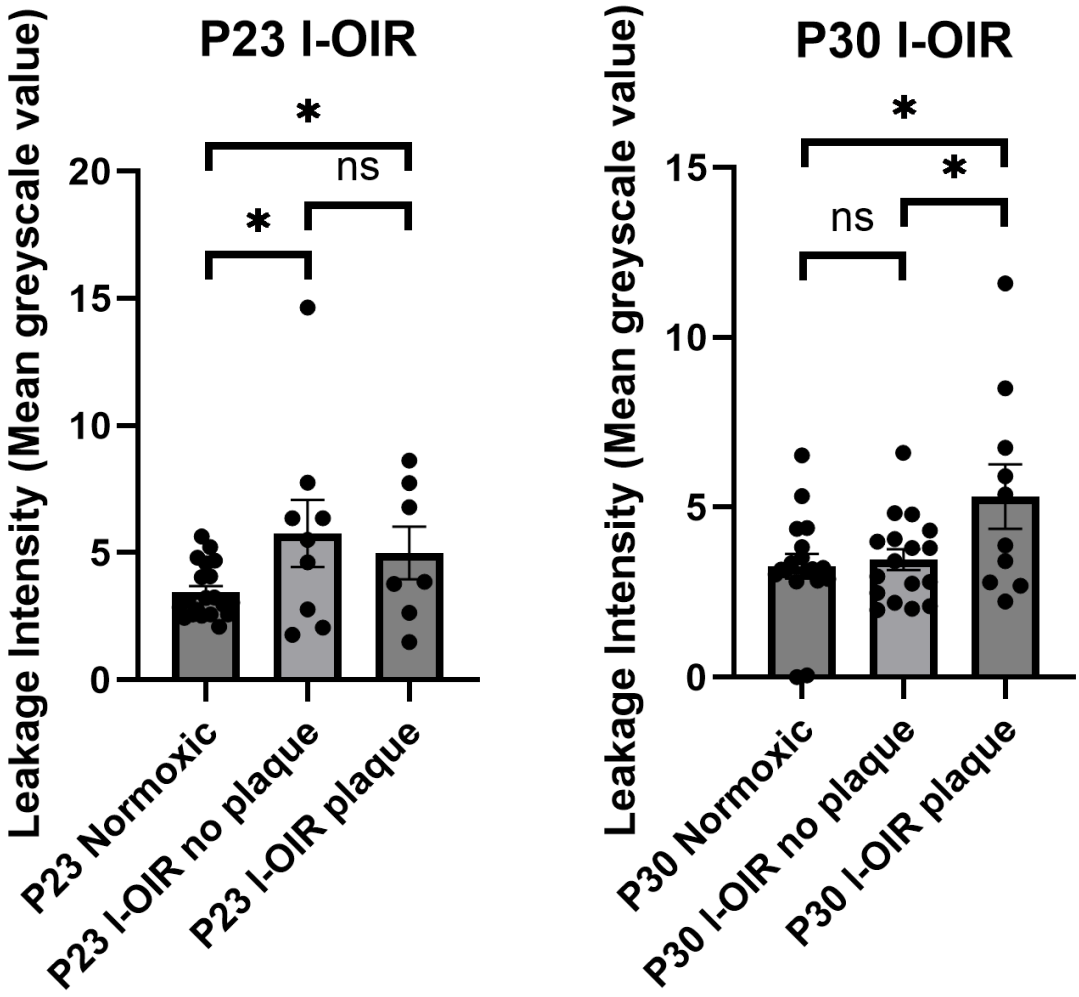

Figure 3: Leakage intensity at P23 and P30 for retinas with and without a fibrotic scar. The l-OIR retinas at P23 and P30 were grouped based on the presence of a scar at each timepoint. P23 l-OIR showed no difference in regard to the presence of a scar. However, P30 l-OIR showed that retinas with a scar leaked, while those without a scar did not. Group comparisons were performed using an unpaired t-test. Each l-OIR group was also compared to the age-matched normoxic group with an unpaired t-test. Leakage intensity was measured in mean greyscale value. *$p<0.05$.

Grouping based on the presence of a scar, the amount of leakage does not correlate with the presence of a scar at P23, but at P30 the scar is associated with leakage. Treatment of mice by l-OIR results in the observation of a scar on some eyes during timepoints P23 and P30. At these timepoints, eyes containing a scar were quantified and the leakage intensity compared to that of eyes without a scar. At P23, there was no statistically significant difference between the amount of leakage in eyes with and without a scar; these groups still had significantly greater leakage than the age-matched normoxic eyes. At P30, however, retinas with a scar leaked significantly more than both the age-matched normoxic and the l-OIR retinas without a scar.

Figures 1, 2, and 3 are being prepared for submission for publication. Nudleman, Eric; Daneman, Richard. The dissertation author is the primary author and researcher of this material.

Discussion

The s-OIR model presents an acute form of ischemic retinal vasculopathy. To visualize the effects that s-OIR has on the retinal vasculature of mice, the sampled retinas were stained with antibodies targeting CD31. The disease progression of the s-OIR model is characterized by vaso-obliteration of the central capillaries, persistence of the central veins and arteries as well as the peripheral capillaries, the formation of neovascular tufts at its most severe stage, and the eventual complete recovery of the retinal vascular network.[14] This characteristic disease progression is seen in Figure 1. At s-OIR P12, when the mice complete the s-OIR high oxygen treatment, the retinas show a central vaso-obliteration of capillaries. At P17, the most severe stage of neovascularization in the s-OIR model, this vaso-obliteration is accompanied by neovascular tufts. By P25, the vasculature shows a return to normal development. When paired with the leakage data, the acute nature of the disease becomes clear, as there is a sharp peak in leakage intensity at P17, while neither P12 nor P25 show any significant leakage.

The l-OIR model presents a chronic form of ischemic retinal vasculopathy. The l-OIR retinas followed the same staining protocol as the s-OIR retinas. While the s-OIR model has distinct stages and a structured timeline for disease progression, the progression of the l-OIR disease state is less uniform. Instead, the l-OIR model takes on a bidirectional progression of disease phenotype, a quicker recovering phenotype with less vaso-obliteration, and a much slower recovering phenotype with severe vaso-obliteration. The most severe l-OIR disease state is characterized by a near complete lack of retinal vasculature. In addition to the central capillaries, vaso-obliteration includes the peripheral capillaries, and central veins and arteries. In contrast to the most severe s-OIR disease state existing at the acute peak of P17, the severe l-OIR disease state was present in a considerable proportion of mice at all timepoints from P16 to P30.

It is because some mice seem to remain in this disease state while others are recovering that the disease progression in l-OIR takes on its bidirectional nature.

Leakage is observed in l-OIR retinas immediately upon removal from the high oxygen environment. In Figure 2, depicting the normalized leakage intensities, the contrast between the acute nature of s-OIR versus chronicity of l-OIR becomes clear. Unlike the P12 s-OIR retinas, at P16, l-OIR retinas show a significant amount of leakage in comparison to the age-matched normoxic retinas. This leakage has a small peak at P19 and persists through P23, exhibiting a much more chronic form of progression. Despite some mice still suffering from a severe disease state at P30, the overall leakage of intensity was no longer statistically different from those of the age-matched normoxic retinas. This indicates that while the disease has the potential to persist to this point, most of the mice are recovering as they near the 2-week mark.

The severe vaso-obliteration of l-OIR leads to leakage occurring peripherally as well as centrally. One of the biggest differences between s-OIR and l-OIR is the behavior of the central veins and arteries. In mice treated with s-OIR, the central veins and arteries can be seen flowing directly to the periphery before branching into capillaries. In l-OIR, there are instances where a single central vessel, sometimes two, flows into the periphery and, rather than branching into capillaries, circumscribes the peripheral region of the retina. In cases, this circumscribing vessel is observed leaking into the periphery, something not observed in s-OIR. Furthermore, the disease produced by l-OIR can be seen generating vascular structures with peripheral capillaries and no central veins or arteries. One reason that the l-OIR model seems to leak less than the s-OIR model is the difference in vascular structure during disease. The majority of leakage intensity is localized to the central vessels and the tissue surrounding them. Without these big

vessels to bring fluid to the retina, the l-OIR retinas may not have the necessary infrastructure to produce large amounts of leakage.

Extreme atrophy of retinal tissue may be reducing leakage. Vascular endothelial growth factor (VEGF) plays a critical role in the development of a healthy retinal vasculature. As shown in the Smith et al. model, placement of infant mice into a high-oxygen environment results in a sharp decline in VEGF production, leading to the characteristic vaso-obliteration of the s-OIR model.[8] Upon removal from high oxygen, VEGF is upregulated, causing the observed neovascularization and leakage. This is important because a multitude of retinal cells are involved in the synthesis of VEGF, including but not limited to Müller cells, glial cells, and pericytes, with Müller cells suspected to play a large role in pathological angiogenesis.[15, 16] Notably, total ischemia has been found to be particularly fatal for Müller cells due to an ischemia-induced glutathione deficiency and the heavy presence of reactive oxygen species during this condition.[17] As such, the lower amount of leakage observed in l-OIR may be because the model causes such a severe form of ischemia that the extreme tissue atrophy reduces VEGF signaling and response. One way to determine this would be to perform transcriptomics on the retinal cells to identify which factors are upregulated during the l-OIR disease state. This may differ depending on the severity of the disease. Further experimentation may include identifying which cells atrophy via cell specific markers allowing for deeper insights into how the VEGF response on both a cellular and molecular level is potentially altered due to scarring.

P30 l-OIR with a scar leaks. In Figure 4, grouping the P30 retinas based on the presence of a scar shows that retinas with a scar leak, while those with no scar do not. Although this may seem to contradict the current understanding of retinal scar formation - scarring is typically

associated with a reduction in leakage - the samples with a scar all show continued neovascularization, whereas most of those without a scar show a recovered vasculature.[18] Therefore, it is likely that the scar is a symptom of a more severe disease phenotype that exhibits much longer-term leakage rather than the cause of the long-term leakage. This shows a lot of promise in the l-OIR model to produce retinal fibrosis similar to what is seen in humans - chronic ischemic vascular diseases that result in the accumulation of a fibrotic scar. As such, the l-OIR model has strong potential to fulfill the need for a retinal fibrosis model, providing the necessary foundation for the advancement of therapeutics and patient standard of care. However, critical to this is expanding upon the understanding of the model first. An important distinction to make regarding scarring as it relates to leakage is that the mouse retina possesses the ability to fully recover from the oxygen-induced damage. Human retinas do not. This makes it difficult to draw strong parallels between scar related leakage within the mouse model and human clinical conditions based on leakage data alone. Further experimentation such as performing electroretinography to determine functional changes caused by scarring in the l-OIR model and comparing to the s-OIR model or cryosectioning samples to determine tissue structure underlying the scar would provide greater insights into the pathophysiology of scarring in the l-OIR model.

References

1. Wynn TA. Cellular and molecular mechanisms of fibrosis. *J Pathol*. 2008;214(2):199-210. doi:10.1002/path.2277

2. Schuppan D, Ruehl M, Somasundaram R, Hahn EG. Matrix as a modulator of hepatic fibrogenesis. *Semin Liver Dis*. 2001;21(3):351-372. doi:10.1055/s-2001-17556

3. Friedlander M. Fibrosis and diseases of the eye. *J Clin Invest*. 2007;117(3):576-586. doi:10.1172/JCI31030

4. Cho C, Wang Y, Smallwood PM, Williams J, Nathans J. Dlg1 activates beta-catenin signaling to regulate retinal angiogenesis and the blood-retina and blood-brain barriers. *Elife*. 2019;8:e45542. Published 2019 May 8. doi:10.7554/eLife.45542.

5. Kumar, A., Mohanraj, S.N., Duraipandi, K., Pai, A.V. Antiangiogenic Agents and Photodynamic Therapy. 2016 March. In: Velpandian, T. (eds) Pharmacology of Ocular Therapeutics. Adis, Cham. https://doi.org/10.1007/978-3-319-25498-2_9

6. Snead D., James S, Snead MP. Pathological changes in the vitreoretinal junction 1: epiretinal membrane formation. *Eye (Lond)*. 2008;22(10):1310-1317. doi:10.1038/eye.2008.36

7. Thannickal VJ, Zhou Y, Gaggar A, Duncan SR. Fibrosis: ultimate and proximate causes. *J Clin Invest*. 2014;124(11):4673-4677. doi:10.1172/JCI74368

8. Smith LE, Wesolowski E, McLellan A, Kostyk SK, D'Amato R, Sullivan R, D'Amore PA. Oxygen-induced retinopathy in the mouse. *Invest Ophthalmol Vis Sci*. 1994;35(1):101-111.

9. Gilbert C. Retinopathy of prematurity: a global perspective of the epidemics, population of babies at risk and implications for control. *Early Hum Dev*. 2008;84(2):77-82. doi:10.1016/j.earlhumdev.2007.11.009

10. Hughes S, Yang H, Chan-Ling T. Vascularization of the human fetal retina: roles of vasculogenesis and angiogenesis. *Invest Ophthalmol Vis Sci*. 2000;41(5):1217-1228.

11. Sapieha P, Joyal JS, Rivera JC, Kermorvant-Duchemin E, Sennlaub F, Hardy P, Lachapelle P, Chemtob S. Retinopathy of prematurity: understanding ischemic retinal vasculopathies at an extreme of life. *J Clin Invest*. 2010;120(9):3022-3032. doi:10.1172/JCI42142

12. Trese MT, Droste PJ. Long-term postoperative results of a consecutive series of stages 4 and 5 retinopathy of prematurity. *Ophthalmology*. 1998;105(6):992-997. doi:10.1016/S0161-6420(98)96024-9

13. Wynn TA, Ramalingam TR. Mechanisms of fibrosis: therapeutic translation for fibrotic disease. *Nat Med*. 2012;18(7):1028-1040. Published 2012 Jul 6. doi:10.1038/nm.2807

14. Selvam S, Kumar T, Fruttiger M. Retinal vasculature development in health and disease. *Prog Retin Eye Res*. 2018;63:1-19. doi:10.1016/j.preteyeres.2017.11.001.

15. Simó R, Carrasco E, García-Ramírez M, Hernández C. Angiogenic and antiangiogenic factors in proliferative diabetic retinopathy. *Curr Diabetes Rev*. 2006;2(1):71-98. doi:10.2174/157339906775473671

16. Bai Y, Ma JX, Guo J, Wang J, Zhu M, Chen Y, Le YZ. Müller cell-derived VEGF is a significant contributor to retinal neovascularization. *J Pathol*. 2009;219(4):446-454. doi:10.1002/path.2611

17. Huster D, Reichenbach A, Reichelt W. The glutathione content of retinal Müller (glial) cells: effect of pathological conditions. *Neurochem Int*. 2000;36(4-5):461-469. doi:10.1016/s0197-0186(99)00149-7

18. Tenbrock L, Wolf J, Boneva S, Schlecht A, Agostini H, Wieghofer P, Schlunck G, Lange C. Subretinal fibrosis in neovascular age-related macular degeneration: current concepts, therapeutic avenues, and future perspectives. *Cell Tissue Res*. 2022;387(3):361-375. doi:10.1007/s00441-021-03514-8